

Published in final edited form as:

Neuron. 2015 January 7; 85(1): 60–67. doi:10.1016/j.neuron.2014.11.026.

Stoichiometry and phosphoisotypes of hippocampal AMPA type glutamate receptor phosphorylation

Tomohisa Hosokawa¹, Dai Mitsushima^{2,3}, Rina Kaneko¹, and Yasunori Hayashi^{1,4,*}

¹Brain Science Institute, RIKEN, Wako, Saitama 351-0198, Japan

²Department of Physiology, Yokohama City University Graduate School of Medicine, Yokohama Kanagawa 236-0004, Japan

³Department of Systems Neuroscience, Yamaguchi University Graduate School of Medicine, Ube, Yamaguchi 755-8505 Japan

⁴Saitama University Brain Science Institute, Saitama University, Saitama 338-8570 Japan

SUMMARY

It has been proposed that the AMPAR phosphorylation regulates trafficking and channel activity, thereby playing an important role in synaptic plasticity. However, the actual stoichiometry of phosphorylation, information critical to understand the role of phosphorylation, is not known because of the lack of appropriate techniques for measurement. Here, using Phos-tag SDS-PAGE, we estimated the proportion of phosphorylated AMPAR subunit GluA1. The level of phosphorylated GluA1 at S831 and S845, two major sites implicated in AMPAR regulation, is almost negligible. Less than 1% of GluA1 is phosphorylated at S831 and less than 0.1% at S845. Considering the number of AMPAR at each synapse, the majority of synapses do not contain any phosphorylated AMPAR. Also, we did not see evidence of GluA1 dually phosphorylated at S831 and S845. Neuronal stimulation and learning increased phosphorylation but the proportion was still low. Our results impel us to reconsider the mechanisms underlying synaptic plasticity.

INTRODUCTION

The phosphorylation of AMPAR has been proposed to play a critical role in synaptic plasticity (Derkach et al. 2007; Shepherd and Huganir 2007). The hypothesis involves the phosphorylation of AMPAR subunit GluA1 in a two-step process. Phosphorylation of S845 by PKA is a prerequisite for triggering AMPAR trafficking to the synaptic surface and maintenance during basal transmission (Lee et al. 2000; Esteban et al. 2003; Oh et al. 2006). Potentiation of synaptic transmission takes place when the receptor is additionally phosphorylated at S831 by CaMKII. This phosphorylation increases the single channel

© 2014 Elsevier Inc. All rights reserved.

*Correspondence: yhayashi@brain.riken.jp.

Publisher's Disclaimer: This is a PDF file of an unedited manuscript that has been accepted for publication. As a service to our customers we are providing this early version of the manuscript. The manuscript will undergo copyediting, typesetting, and review of the resulting proof before it is published in its final citable form. Please note that during the production process errors may be discovered which could affect the content, and all legal disclaimers that apply to the journal pertain.

conductance and contributes to the increased transmission following LTP induction (Benke et al. 1998; Derkach et al. 1999; Banke et al. 2000). In contrast, LTD is mediated by receptor removal caused by the dephosphorylation of S845-phosphorylated GluA1 at the synaptic surface (Kameyama et al. 1998; Lee et al. 2000). Overall, this scheme assumes that a large proportion of the GluA1 mediating synaptic transmission is phosphorylated. If LTP is maintained by phosphorylation of GluA1 at S831 and S845, one should be able to find dually phosphorylated GluA1 at these sites after LTP induction. Likewise, if dephosphorylation triggers removal of surface AMPAR during LTD, the majority of GluA1 maintaining basal transmission should be phosphorylated at S845. Phosphorylation at S818 controls the interaction with Band 4.1N, a cytoskeletal anchoring protein and those at T840 and S567 are also implicated in synaptic plasticity (Boehm et al. 2006; Delgado et al. 2007; Lee et al. 2007; Lu et al. 2010). Hence, multiple phosphorylation on GluA1 has been suggested to cooperatively participate in the induction and maintenance of synaptic plasticity.

However, critical information to attest this scheme, the stoichiometry of GluA1 phosphorylation and the phosphoisotypes (combination of phosphorylated sites) involved, are unknown. Several methods, including phosphospecific antibodies, phosphopeptide mapping and mass spectrometry, have been used to detect the phosphorylation of specific sites. However, using these approaches, it is difficult to determine the proportion of phosphorylation and the phosphoisotypes. For example, western blotting with a phosphospecific antibody can detect a doubling of phosphorylation. However, it cannot distinguish whether the change is from 0.1% to 0.2% or from 10% to 20%. Also, it is very difficult to determine the phosphoisotype using phosphospecific antibodies. Because of this, although dually phosphorylated GluA1 at S831 and S845 is implicated in LTP, the presence of such receptor molecules have not been demonstrated. Therefore, critical experimental evidence to verify the aforementioned scheme is still lacking.

Phos-tag is a compound that associates with phosphate groups on a protein in the presence of divalent cations (Kinoshita et al. 2008; Hosokawa et al. 2010). When covalently conjugated with polyacrylamide in a SDS-PAGE, it separates phosphorylated from unphosphorylated proteins. Because the extent of separation is dependent on both the number of phosphorylated residues and the surrounding sequence, one can separate distinct phosphoisotypes of a given protein based on mobility. Furthermore, by blotting the gel with an appropriate antibody, one can also determine the stoichiometry of different phosphoisotypes.

Using this feature of Phos-tag SDS-PAGE, we quantified GluA1 phosphorylation in both mature and developing hippocampus. We found that the stoichiometry of phosphorylation in adult tissue is much lower than expected from the current plasticity model. We did not find any evidence of GluA1 dually phosphorylated at both S831 and S845. Our results compel us to re-evaluate the current model of AMPAR regulation.

RESULTS

Phos-tag SDS-PAGE separates GluA1 phosphorylated at different sites

To test whether Phos-tag SDS-PAGE is applicable for the analysis of GluA1 phosphoisotypes, GluA1 was expressed in HEK293T cells and phosphorylation was induced by blocking endogenous phosphatase activity with okadaic acid (OA), an inhibitor of protein PP1 and 2A. This treatment increased the phosphorylation of various proteins in HEK293T cells (Fig. S1A), likely by unmasking the basal activity of endogenous kinases. While GluA1 on conventional SDS-PAGE did not show a difference in migration in the presence or absence of OA, it showed multiple bands that migrated slowly only in the presence of OA on Phos-tag SDS-PAGE (Fig. 1A). These bands disappeared by treating the cell lysate with λ protein phosphatase (Fig. 1B).

To test whether the band shift was caused by phosphorylation at a previously identified GluA1 site, we mutated all five known phosphorylation sites to alanine (5A, Fig. 1C). The GluA1 wild type or 5A mutant were coexpressed with a constitutively active form of CaMKII (phosphorylates GluA1 at S567 and S831) and the cells were further treated with phorbol ester (PKC activator, S818, S831, and T840), forskolin (PKA activator, S845), cyclosporine A (PP2B inhibitor) and OA (Barria et al. 1997; Lu et al. 2010; Roche et al. 1996; Boehm et al. 2006). Unlike wildtype GluA1, 5A mutants did not show a band shift indicating that there were no other phosphorylation sites under this condition.

To identify the phosphorylation sites causing the band shift, we mutated each of the alanine residues back to serine or threonine, while maintaining the other 4 alanines (4A mutants). S831, T840, and S845 on a 4A background showed a clear band shift but at different positions. They were confirmed to be GluA1 phosphorylated at respective sites by blotting with phosphoantibodies. In contrast, S567 or S818 on a 4A background did not show a noticeable band shift. Also, an antibody against pS567 (Lu et al. 2010) did not detect any phosphorylated proteins, indicating a low phosphorylation stoichiometry (not shown). As a result, we did not investigate the S567 and S818 phosphorylation sites further and focused on S831, T840 and S845.

To test if GluA1 dually phosphorylated at S831 and S845 could be detected, we made a construct that maintained both S831 and S845, but mutated the other three sites to alanine (Fig. 1D, 3A 831+845). Blotting with a C-terminus antibody detected GluA1 phosphorylated at S831, S845, as well as unphosphorylated protein. Additionally, we detected a band above S831, which was confirmed to be dually phosphorylated GluA1 in the blots with pS831 and pS845 antibodies. This band was at almost the same location as singly phosphorylated GluA1 at T840. Therefore, for the rest of study, we routinely reblotted the membrane with phosphospecific antibodies to identify the phosphoisotype of each band.

Likewise, both individually and dually phosphorylated GluA1 were detected in S831 and T840 on a 3A background (the T840 band could be visualised using the C-terminus antibody but was too faint in the pT840 blot. Fig. 1D). In the T840 and S845 on a 3A background, individually phosphorylated bands but not dually phosphorylated bands were detected. In

summary, Phos-tag SDS-PAGE in combination with phosphospecific antibodies allows us to detect the phosphoisotypes of singly and dually phosphorylated GluA1.

Estimation of phosphorylation stoichiometry using Phos-tag SDS-PAGE

Next we tested if we could use Phos-tag SDS-PAGE to determine the stoichiometry of GluA1 phosphorylation. For this purpose, we first ascertained whether the GluA1 C-terminus antibody detects each phosphoisotype with equal efficiency. We maximally phosphorylated GluA1 mutants 5A or S831, T840, and S845 on 4A background and tested the reactivity of the antibody (Fig. 1E). Phos-tag SDS-PAGE confirmed that they were ~100% phosphorylated. In these samples, there were no obvious differences in band intensity between the 5A and phosphorylated mutants, confirming that phosphorylation at S831, T840 and S845 did not affect the reactivity of the C-terminus antibody.

We therefore assumed that, by comparing the intensity of the bands corresponding to phosphorylated and unphosphorylated GluA1 in the blot with C-terminus antibody, we could estimate the stoichiometry of GluA1 phosphorylation using Phos-tag SDS-PAGE. To test this, we compared the result of quantification using Phos-tag SDS-PAGE with that of mass spectrometric absolute quantification (AQUA) (Gerber et al. 2003). We immunoprecipitated GluA1 (S831 on 4A background) from HEK293T cells, untreated or treated with okadaic acid and mixed them at different ratios, thereby making a series of GluA1 samples with different stoichiometry of S831 phosphorylation. The stoichiometry of S831 phosphorylated GluA1 in each mixture was determined by western blotting with the C-terminus antibody and measuring the band intensity of S831 phosphorylated and unphosphorylated GluA1 on the Phos-tag SDS-PAGE (Fig. 1F). In parallel, the same samples were subjected to AQUA using a synthetic standard of phosphorylated and unphosphorylated peptides containing ^{13}C and ^{15}N (Fig. S1D). The results from these two methods coincide with each other precisely (Fig. 1G), indicating that Phos-tag SDS-PAGE is a reliable measure of the stoichiometry of protein phosphorylation.

Quantitative analysis of GluA1 phosphorylation in hippocampus

We next determined the amount of phosphorylated GluA1 in adult rat hippocampus. In conventional SDS-PAGE, blotting with antibodies against GluA1 C-terminal, pS831, pT840 and pS845 showed bands at the expected molecular weight (Fig. 2A, top). As expected, upon phosphatase treatment, the bands disappeared from the blots using phosphoantibodies. Using Phos-tag SDS-PAGE, we observed a discrete band shift with pS831, pT840 and pS845 antibodies at similar relative positions as HEK293T cells (Fig. 2A, bottom). However, when blotting was performed with the C-terminus antibody, <1% of pS831 and ~5% of pT840 GluA1 were detected at the corresponding positions and pS845 was undetectable (Fig. 2A bottom, B and C). The dually phosphorylated GluA1 at S831 and S845 is expected to be at almost the same location as T840 phosphorylated GluA1 (Fig. 1D), but, as there was no signal on the pS831 and pS845 blots (Fig. 2A), we concluded that the upper band in the blot with C-terminal antibody was composed solely of pT840 GluA1. Likewise, there was no evidence of other multiply phosphorylated GluA1.

We also subjected hippocampal GluA1 to AQUA. Consistent with the result of Phos-tag SDS-PAGE, it also showed that pS831 on GluA1 from hippocampal tissue was barely detectable, an amount that was significantly lower than the smallest standard (2.3%) (Fig. S1D). Changes in sample preparation method did not change the level of phosphorylation (Fig. S2A). Therefore it is unlikely that GluA1 is dephosphorylated during sample preparation.

To further extend the dynamic range, we calibrated the immunoblot signal as follows. The 4A mutant samples containing ~100% phosphorylated receptors (Fig. 1E) were serially diluted, separated using conventional SDS-PAGE, and blotted with phosphoantibodies, from which a calibration line was drawn (Fig. 2D, E). Hippocampal extract, preadjusted so that it contains the same amount of total GluA1 (Fig. 2D bottom), was also separated on the same gel and the amount of phosphorylated GluA1 at each site was obtained from the calibration line (Fig. 2D top, E). We estimated that $0.18 \pm 0.01\%$, $4.3 \pm 0.7\%$ and $0.018 \pm 0.001\%$ of hippocampal GluA1 was phosphorylated at S831, T840 and S845, respectively (Fig. 2D, E), largely consistent with the measurement of band intensity on Phos-tag SDS-PAGE.

One reason why only a small proportion of phosphorylated GluA1 was detected may be because the extract is a mixture of various membranous compartments. We therefore extracted the PSD fraction by detergent treatment, which is enriched with PSD-95, a prominent PSD protein, but lacks synaptophysin, a presynaptic protein (Fig. 2F). Phos-tag SDS-PAGE revealed that the phosphorylation of GluA1 was not significantly different from other fractions. We also attempted to isolate surface GluA1 from cultured hippocampal neurons using a surface biotinylation and avidin pull-down (Fig. 2G). There was no obvious difference in phosphoisotypes between internal and surface GluA1.

We next tested the ontogeny of GluA1 phosphorylation. The GluA1 phosphorylation was highest at P1 (Fig. 2H, I). This was evident for pS831, which was 36.2 ± 1.3 fold higher at P1 compared with adult tissue. The level gradually diminished during development and reached adult levels by P28. We found that ~7% and ~25% of GluA1 is phosphorylated at S831 and T840 respectively at P1 (Fig. S2B and C). In addition, ~2.5% of GluA1 was dually phosphorylated at both S831 and T840. However, the level of S845 phosphorylated GluA1 was still low, as indicated by the lack of a band detected by the N-terminal antibody at the corresponding position in the pS845.

We also analyzed other postsynaptic proteins in the hippocampus (Fig. S2D). We found that a significant proportion of GluN2B was phosphorylated at tyrosine sites in both P1 and adult hippocampal tissue, though we did not attempt to determine the exact site. Almost all stargazin in adult PSD fraction was phosphorylated, consistent with an earlier study (Sumioka et al. 2010). A minor population of PSD-95 was phosphorylated in adult tissue; possibly at S73 or S295 (Kim et al. 2007; Steiner et al. 2008). Likewise, a minor population of cofilin was phosphorylated at S3 both in P1 and adult tissue. These data demonstrate the versatility of Phos-tag SDS-PAGE in estimating the stoichiometry of phosphorylation of various proteins.

GluA1 phosphorylation in chemical LTP

We next attempted to test if the level of GluA1 phosphorylation changes by stimulating neurons. We induced chemical LTP (chemLTP) in dissociated neuronal cultures by applying a saturating concentration of glycine (Lu et al. 2001). Following the stimulation, the levels of surface GluA1 was increased by 1.43 ± 0.12 -fold (Fig. 3A, B) as reported (Lu et al. 2001). Concomitantly, pS831 and pS845 GluA1 on the cell surface increased significantly beyond the increase in total surface GluA1, indicating a net increase in the proportion of phosphorylated GluA1 (Fig. 3A–C). However, the proportion of phosphorylated cell surface GluA1 still remained low, from $0.16 \pm 0.02\%$ before stimulation to $0.25 \pm 0.02\%$ after chemLTP induction at S831, and $0.012 \pm 0.001\%$ to $0.047 \pm 0.002\%$ at S845 (Fig. 3D–F).

The low amount of phosphorylated GluA1 may be due to rapid dephosphorylation. We therefore, treated the cells with phosphatase inhibitors. Treatment of unstimulated neurons lead to a significant increase in phosphorylated receptors (Fig. 3A, C, D, S3A). This was mostly due to pT840, which increased by 19.1 ± 7.3 fold of basal levels and reached ~80 % of the total GluA1, indicating that T840 is undergoing a constant phosphorylation-dephosphorylation cycle during basal states (Fig. 3A, C, D, S3). pS831 increased by 7.54 ± 0.81 fold and pS845 by 2.54 ± 0.31 fold (Fig. 3A, C, S3B) but they still only account for a small proportion (Fig. S3C). Also, treatment with the phosphatase inhibitor itself did not increase surface GluA1 levels (Fig. 3A, B).

When phosphatase inhibitors were combined with glycine, it increased the surface GluA1 by 2.31 ± 0.25 -fold, whilst the increase was only 1.43 ± 0.12 -fold with glycine alone (Fig. 3A, B). However, the effect on phosphorylation of cell surface GluA1 was still small. pS831 and pT840 did not increase further and S845 marginally increased (Fig. 3C, D). In summary, T840 undergoes cycles of phosphorylation-dephosphorylation under basal conditions, with endogenous phosphatase activity maintaining phosphorylation at low levels. In contrast, the kinase activity to phosphorylate S831 and S845 is intrinsically low, at both basal states and during chemLTP induction and it is not phosphatase activity that maintains low levels of phosphorylation.

GluA1 phosphorylation in inhibitory avoidance learning

To examine GluA1 phosphorylation *in vivo*, PSD fractions of hippocampal tissue from rats that underwent inhibitory avoidance learning was analyzed. This paradigm induces a rapid and persistent potentiation of hippocampal synaptic transmission both *in vitro* and *in vivo* (Whitlock et al. 2006; Mitsushima et al. 2011; 2013). We found a 2.5 fold increase in AMPA/NMDA ratio, a 33% increase in miniature EPSC amplitude and a 54% increase in frequency in randomly sampled cells compared with tissue from control animals, indicating that a significant proportion of synapses undergo potentiation with this paradigm. We prepared PSD fractions from rats before, 5 min and 30 min after training, when an increase in transmission was observed. The training induced an increase in pS831 and pS845 GluA1 in the PSD fraction, consistent with earlier studies (Whitlock et al. 2006; Mitsushima et al. 2011) but not in pT840 (Fig. 4A, B). However, when compared with the total levels of GluA1 in the PSD fraction, the amount of phosphorylated GluA1 at these sites was still low

(Fig. 4C–E). It was $0.21 \pm 0.02\%$ under basal conditions and $0.33 \pm 0.01\%$ 30 min after learning for S831 and $0.023 \pm 0.004\%$ and $0.044 \pm 0.004\%$ for S845.

DISCUSSION

The stoichiometry of phosphorylation and phosphoisotypes of GluA1, two critical pieces of information to attest the importance of AMPAR phosphorylation in synaptic plasticity, have been overlooked so far, in part due to the lack of an appropriate method to obtain such information. Using Phos-tag SDS-PAGE, we found that the amount of phosphorylated GluA1 was very low. In naïve hippocampal tissue, 0.18% and 0.018% of GluA1 was phosphorylated at S831 and S845, respectively. If we assume that there are 100 GluA1 molecules on each synapse (Tanaka et al. 2005; Sheng and Hoogenraad 2007), on average, only 1 out of ~6 of synapses contain single pS831 GluA1 and 1 out of ~60 for pS845. Hence, the majority of GluA1 at synapses are not phosphorylated and the rest of the synapses do not contain any phosphorylated GluA1. We also saw no evidence of dually phosphorylated GluA1 at S831 and S845.

In light of these results, the current model of plasticity, which assumes AMPAR phosphorylation plays a significant role, needs to be re-evaluated. First, it is difficult to explain how LTP maintenance is linked with an increase in phosphorylation. GluA1 phosphorylation at S831 increases channel conductance only by ~two fold (Derkach et al. 1999). Such an effect would be diluted by unphosphorylated AMPARs, which make up the majority of the AMPAR population. One possibility is that transient phosphorylation might be sufficient to induce LTP. However, we ruled out this possibility by treatment with a phosphatase inhibitor, which only marginally increased S831 and S845 phosphorylation upon glycine treatment. Similarly, the majority of synapses do not contain even a single S845-phosphorylated GluA1. This observation rules out the possibility that LTD is mediated by dephosphorylation of synaptic GluA1.

Our estimation is in contrast with Oh et al. (2006) who found that ~15% of surface AMPARs were phosphorylated at S845 during basal conditions and increased to ~60% following chemLTP. They used a GST-fusion protein of GluA1 C-terminus, phosphorylated to ~100%, as a standard. However, they introduced a P842R mutation to make it an efficient substrate of PKA. This manipulation may change the antigenicity of the fusion protein to the pS845 antibody and cause inaccuracy. Also, quantification of pS845 with the incorporation of ^{32}P may be compromised by possible phosphorylation at other sites, for example T840. Finally, to induce chemLTP, they used forskolin/rolipram, which stimulates PKA, whereas we stimulated NMDA receptors with glycine.

T840 was the only site whereby a significant proportion of GluA1 was phosphorylated. However, glycine treatment only slightly increased pT840 GluA1 (1.27 ± 0.17 fold, statistically insignificant) and inhibitory avoidance training did not affect pT840 level. Even though we saw a ~20-fold increase in pT840 level after treatment with a phosphatase inhibitor, it still did not change the amount of cell surface GluA1. Also, T840A knock-in animals, with S838A, S839A and additional S831A/S845A mutations, did not show any

further phenotype compared with S831A/S845A knock-in (Lee et al. 2007). Therefore, the functional significance of this phosphorylation requires further study.

The impairment of synaptic plasticity in the S831A/S845A knock-in mutant GluA1 mice is generally accepted as strong evidence supporting the requirement of receptor phosphorylation (Lee et al. 2003). Studies using exogenous mutant receptors support this view (Esteban et al. 2003; Miyazaki et al. 2012; but see Hayashi et al. 2000). We indeed observed a significant increase in phosphorylation at S831 and S845 along with an increase in the surface GluA1 as a result of chemLTP or learning (Fig. 3 and 4). Therefore, we need to find alternative interpretations for the role of GluA1 phosphorylation. Firstly, phosphorylation in a small proportion of GluA1 may be sufficient to trigger changes in the population of unphosphorylated AMPAR. Alternatively, GluA1 phosphorylation may be important for normal synaptic development, when the GluA1 phosphorylation levels were high (Fig. 2H) (Li et al. 2003). Impairment of the process may later manifest as an impairment in synaptic plasticity. Finally, these residues may be required for other protein interactions or forms of posttranslational modification. Recently, it was proposed that LTP does not require the carboxyl-tail of AMPA receptor GluA1 and GluA2 with a distinct carboxyl-tail lacking these phosphorylation sites can replace GluA1 (Granger et al. 2013). Together, these results compel us to consider what is the true mechanism of synaptic plasticity.

METHODS AND MATERIALS

Phos-tag SDS-PAGE

Four % acrylamide gel strengthened with 0.2 % or less agarose was mixed with 25 μ M Phos-tag acrylamide (AAL-107, Wako) and 25 μ M $MnCl_2$. After sample separation, the gel was washed with blotting buffer containing 20 mM EDTA for one hour to chelate Mn^{2+} . Proteins were transferred to PVDF membrane and used for blotting. We confirmed the complete transfer by staining the remaining gel with CBB staining or blotting with the second PVDF membrane. The signal was detected with ECL Prime Western Detection Reagents (GE Healthcare) on LAS 3000 (Fujifilm).

Supplementary Material

Refer to Web version on PubMed Central for supplementary material.

Acknowledgments

We thank Akane Shibuya and Yuki Okumura-Takayagi for assistance and Drs. Katherine Roche, Roger Nicoll, Takeo Saneyoshi, Kaori Otsuki, Masaya Usui, Eiji Kinoshita, Takuya Takahashi, Masaki Matsumoto, Takashi Hayashi, Steve Heinemann, John Lisman, and Lily Yu for sharing resources and comments on the manuscript. This work was supported by RIKEN, NIH grant R01DA17310, Grant-in-Aid for Scientific Research (A) and Grant-in-Aid for Scientific Research on Innovative Area "Foundation of Synapse and Neurocircuit Pathology" from the MEXT, Japan (Y.H.).

References

- Banke TG, Bowie D, Lee H, Huganir RL, Schousboe A, Traynelis SF. Control of GluR1 AMPA receptor function by cAMP-dependent protein kinase. *J Neurosci*. 2000; 20:89–102. [PubMed: 10627585]
- Barria A, Derkach V, Soderling T. Identification of the Ca²⁺/calmodulin-dependent protein kinase II regulatory phosphorylation site in the α -amino-3-hydroxy-5-methyl-4-isoxazole-propionate-type glutamate receptor. *J Biol Chem*. 1997; 272:32727–30. [PubMed: 9407043]
- Benke TA, Lüthi A, Isaac JT, Collingridge GL. Modulation of AMPA receptor unitary conductance by synaptic activity. *Nature*. 1998; 393:793–7. [PubMed: 9655394]
- Boehm J, Kang MG, Johnson RC, Esteban J, Huganir RL, Malinow R. Synaptic incorporation of AMPA receptors during LTP is controlled by a PKC phosphorylation site on GluR1. *Neuron*. 2006; 51:213–25. [PubMed: 16846856]
- Delgado JY, Coba M, Anderson CN, Thompson KR, Gray EE, Heusner CL, Martin KC, Grant SG, O'Dell TJ. NMDA receptor activation dephosphorylates AMPA receptor glutamate receptor 1 subunits at threonine 840. *J Neurosci*. 2007; 27:13210–21. [PubMed: 18045915]
- Derkach V, Barria A, Soderling TR. Ca²⁺/calmodulin-kinase II enhances channel conductance of α -amino-3-hydroxy-5-methyl-4-isoxazolepropionate type glutamate receptors. *Proc Natl Acad Sci U S A*. 1999; 96:3269–3274. [PubMed: 10077673]
- Derkach VA, Oh MC, Guire ES, Soderling TR. Regulatory mechanisms of AMPA receptors in synaptic plasticity. *Nat Rev Neurosci*. 2007; 8:101–13. [PubMed: 17237803]
- Esteban JA, Shi SH, Wilson C, Nuriya M, Huganir RL, Malinow R. PKA phosphorylation of AMPA receptor subunits controls synaptic trafficking underlying plasticity. *Nat Neurosci*. 2003; 6:136–43. [PubMed: 12536214]
- Gerber SA, Rush J, Stemman O, Kirschner MW, Gygi SP. Absolute quantification of proteins and phosphoproteins from cell lysates by tandem MS. *Proc Natl Acad Sci U S A*. 2003; 100:6940–5. [PubMed: 12771378]
- Granger AJ, Shi Y, Lu W, Cerpas M, Nicoll RA. LTP requires a reserve pool of glutamate receptors independent of subunit type. *Nature*. 2013; 493:495–500. [PubMed: 23235828]
- Hayashi Y, Shi SH, Esteban JA, Piccini A, Ponce JC, Malinow R. Driving AMPA receptors into synapses by LTP and CaMKII: Requirement for GluR1 and PDZ domain interaction. *Science*. 2000; 287:2262–2267. [PubMed: 10731148]
- Hosokawa T, Saito T, Asada A, Fukunaga K, Hisanaga S. Quantitative measurement of in vivo phosphorylation states of Cdk5 activator p35 by Phos-tag SDS-PAGE. *Mol Cell Proteomics*. 2010; 9:1133–43. [PubMed: 20097924]
- Kameyama K, Lee HK, Bear MF, Huganir RL. Involvement of a postsynaptic protein kinase A substrate in the expression of homosynaptic long-term depression. *Neuron*. 1998; 21:1163–75. [PubMed: 9856471]
- Kim MJ, Futai K, Jo J, Hayashi Y, Cho K, Sheng M. Synaptic accumulation of PSD-95 and synaptic function regulated by phosphorylation of serine-295 of PSD-95. *Neuron*. 2007; 56:488–502. [PubMed: 17988632]
- Kinoshita E, Kinoshita-Kikuta E, Matsubara M, Yamada S, Nakamura H, Shiro Y, Aoki Y, Okita K, Koike T. Separation of phosphoprotein isotypes having the same number of phosphate groups using phosphate-affinity SDS-PAGE. *Proteomics*. 2008; 8:2994–3003. [PubMed: 18615432]
- Lee HK, Barbarosie M, Kameyama K, Bear MF, Huganir RL. Regulation of distinct AMPA receptor phosphorylation sites during bidirectional synaptic plasticity. *Nature*. 2000; 405:955–9. [PubMed: 10879537]
- Lee HK, Takamiya K, Han JS, Man H, Kim CH, Rumbaugh G, Yu S, Ding L, He C, Petralia RS, et al. Phosphorylation of the AMPA receptor GluR1 subunit is required for synaptic plasticity and retention of spatial memory. *Cell*. 2003; 112:631–43. [PubMed: 12628184]
- Lee HK, Takamiya K, Kameyama K, He K, Yu S, Rossetti L, Wilen D, Huganir RL. Identification and characterization of a novel phosphorylation site on the GluR1 subunit of AMPA receptors. *Mol Cell Neurosci*. 2007; 36:86–94. [PubMed: 17689977]

- Li AJ, Suzuki M, Suzuki S, Ikemoto M, Imamura T. Differential phosphorylation at serine sites in glutamate receptor-1 within neonatal rat hippocampus. *Neurosci Lett*. 2003; 341:41–4. [PubMed: 12676339]
- Lu W, Isozaki K, Roche KW, Nicoll RA. Synaptic targeting of AMPA receptors is regulated by a CaMKII site in the first intracellular loop of GluA1. *Proc Natl Acad Sci U S A*. 2010; 107:22266–71. [PubMed: 21135237]
- Lu W, Man H, Ju W, Trimble WS, MacDonald JF, Wang YT. Activation of synaptic NMDA receptors induces membrane insertion of new AMPA receptors and LTP in cultured hippocampal neurons. *Neuron*. 2001; 29:243–54. [PubMed: 11182095]
- Mitsushima D, Ishihara K, Sano A, Kessels HW, Takahashi T. Contextual learning requires synaptic AMPA receptor delivery in the hippocampus. *Proc Natl Acad Sci U S A*. 2011; 108:12503–8. [PubMed: 21746893]
- Mitsushima D, Sano A, Takahashi T. A cholinergic trigger drives learning-induced plasticity at hippocampal synapses. *Nat Commun*. 2013; 4:2760. [PubMed: 24217681]
- Miyazaki T, Takase K, Nakajima W, Tada H, Ohya D, Sano A, Goto T, Hirase H, Malinow R, Takahashi T. Disrupted cortical function underlies behavior dysfunction due to social isolation. *J Clin Invest*. 2012; 122:2690–701. [PubMed: 22706303]
- Oh MC, Derkach VA, Guire ES, Soderling TR. Extrasynaptic membrane trafficking regulated by GluR1 serine 845 phosphorylation primes AMPA receptors for long-term potentiation. *J Biol Chem*. 2006; 281:752–8. [PubMed: 16272153]
- Roche KW, O'Brien RJ, Mammen AL, Bernhardt J, Haganir RL. Characterization of multiple phosphorylation sites on the AMPA receptor GluR1 subunit. *Neuron*. 1996; 16:1179–88. [PubMed: 8663994]
- Sheng M, Hoogenraad CC. The postsynaptic architecture of excitatory synapses: a more quantitative view. *Annu Rev Biochem*. 2007; 76:823–47. [PubMed: 17243894]
- Shepherd JD, Haganir RL. The cell biology of synaptic plasticity: AMPA receptor trafficking. *Annu Rev Cell Dev Biol*. 2007; 23:613–43. [PubMed: 17506699]
- Steiner P, Higley MJ, Xu W, Czervionke BL, Malenka RC, Sabatini BL. Destabilization of the postsynaptic density by PSD-95 serine 73 phosphorylation inhibits spine growth and synaptic plasticity. *Neuron*. 2008; 60:788–802. [PubMed: 19081375]
- Sumioka A, Yan D, Tomita S. TARP phosphorylation regulates synaptic AMPA receptors through lipid bilayers. *Neuron*. 2010; 66:755–67. [PubMed: 20547132]
- Tanaka J, Matsuzaki M, Tarusawa E, Momiyama A, Molnar E, Kasai H, Shigemoto R. Number and density of AMPA receptors in single synapses in immature cerebellum. *J Neurosci*. 2005; 25:799–807. [PubMed: 15673659]
- Whitlock JR, Heynen AJ, Shuler MG, Bear MF. Learning induces long-term potentiation in the hippocampus. *Science*. 2006; 313:1093–7. [PubMed: 16931756]

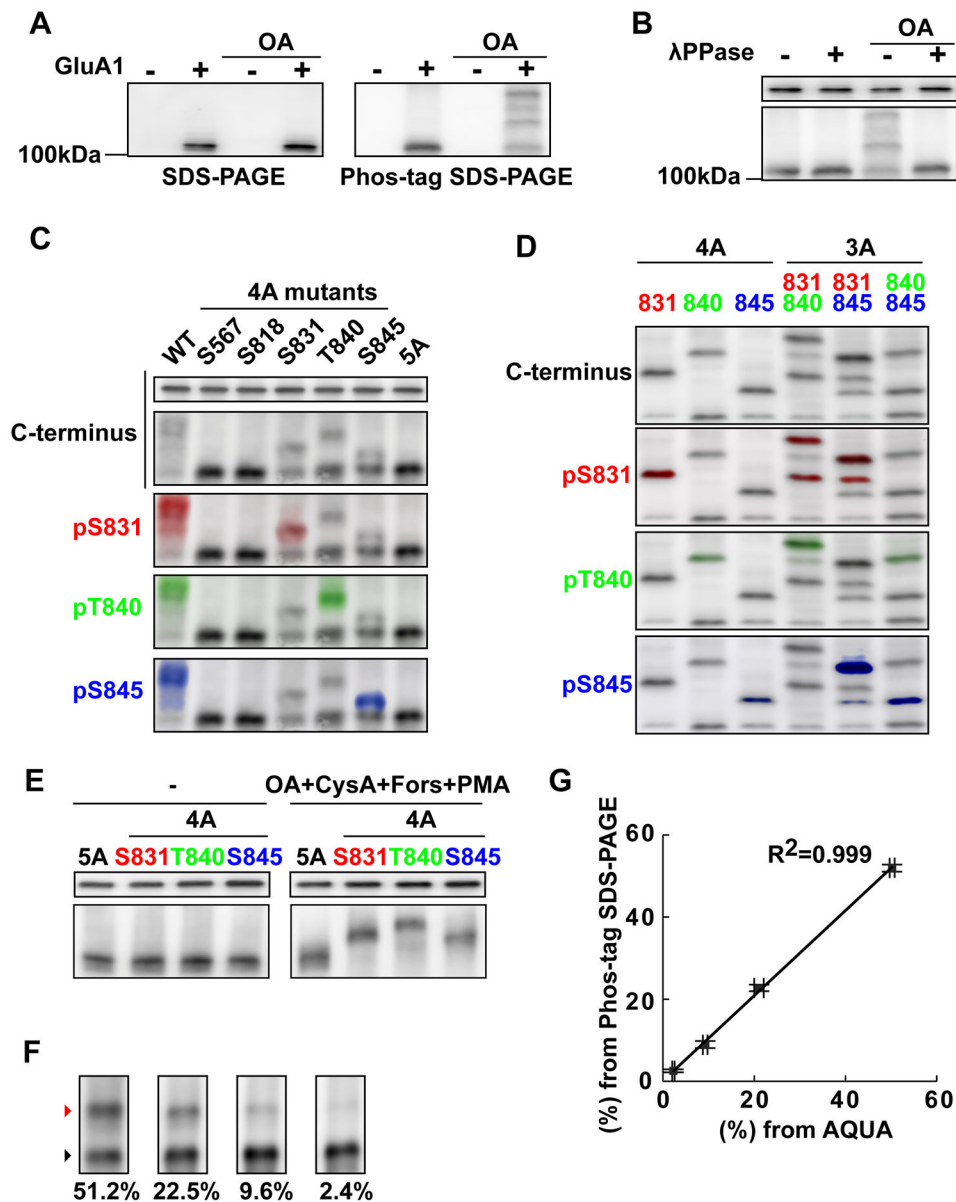


Figure 1. Separation and quantification of phosphoisotypes of GluA1 using Phos-tag SDS-PAGE (A) HEK293T cells expressing GluA1 were incubated with or without 1 μ M okadaic acid (OA) for 4 hrs. The homogenate was separated using conventional (left) or Phos-tag (right) SDS-PAGE and blotted with an antibody against the C-terminus of GluA1. (B) Pre-treatment of the sample with λ protein phosphatase (λ PPase) abolishes the band shift. (C) Wild type (WT) GluA1, 4 alanine mutants (4A) containing mutations in all but one out of five known sites or a mutant where all known phosphorylation sites were mutated to alanine (5A) were expressed in HEK293T cells. To maximally induce phosphorylation, a constitutively active CaMKII was cotransfected and the cells were further treated with forskolin, phorbol 12-myristate 13-acetate, cyclosporine A and okadaic acid for 2 hours. The

cell homogenate was separated using Phos-tag SDS-PAGE and blotted with antibodies against GluA1 C-terminus, pS831, pT840 and pS845.

(D) Detection of dually phosphorylated GluA1. 4A and 3 alanine (3A) mutants were expressed in HEK293T cells and phosphorylated as in (C). The numbers above the blot indicate phosphorylatable sites.

(E) Sensitivity of C-terminus antibody to phosphorylated GluA1. HEK293T cells expressing indicated mutants were treated as in (C) but for a longer duration (6 hours) to ensure complete phosphorylation. Then either unphosphorylated (left) or phosphorylated (right) AMPARs were separated using conventional SDS-PAGE (top) or Phos-tag SDS-PAGE (bottom) and blotted with the C-terminus antibody.

(F) GluA1 samples containing different amounts of pS831 GluA1 (on a 4A background) made by mixing different amounts of immunoprecipitated GluA1 from transfected HEK293T cells untreated or treated with okadaic acid. The mixtures were separated on Phos-tag SDS-PAGE and blotted with the C-terminus antibody. The proportion of pS831 GluA1 in each sample is shown. The same samples were subjected to AQUA (Fig. S1B–D). (G) Correlation of the result of Phos-tag SDS-PAGE (F) and AQUA (Fig. S1D) in the stoichiometry of pS831 GluA1. N=3, each.

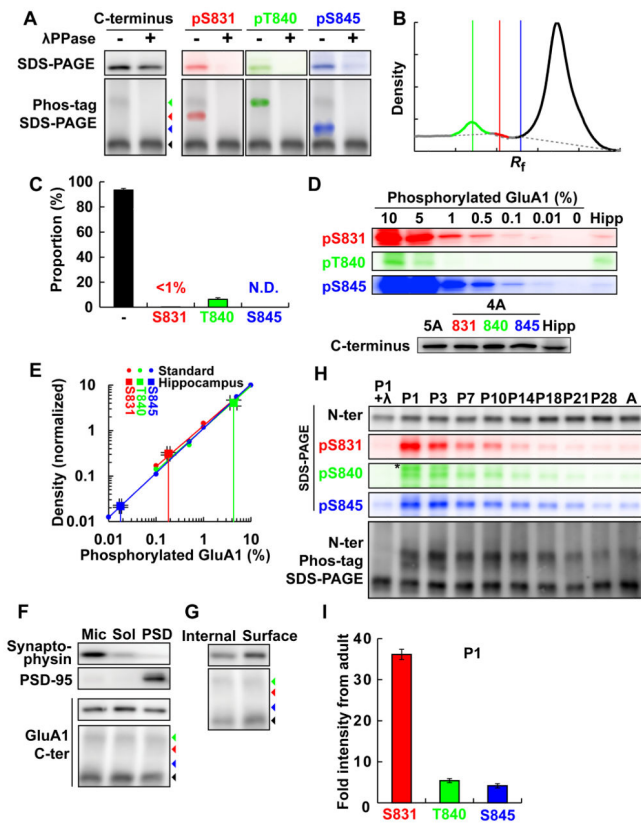


Figure 2. Endogenous GluA1 in neurons is mostly unphosphorylated

(A) Phosphoisotypes of endogenous GluA1 in adult rat hippocampus. Hippocampal extract was subjected to conventional SDS-PAGE (top) or Phos-tag SDS-PAGE (bottom) and blotted with antibodies against GluA1 C-terminus, pS831, pT840 and pS845.

(B) The densitometric profile of blots of hippocampal extract. The positions of pS831, pT840 and pS845 phosphoisotypes are shown by red, green and blue lines respectively.

(C) Quantification of the population of each phosphoisotype. The pS831 was below the level where it could be confidently quantified (<1%) and pS845 was not detected.

(D) Blots of the dilution series of maximally phosphorylated 4A mutants on a conventional SDS-PAGE. Endogenous GluA1 from adult rat hippocampus was loaded on the right lane. Only one rat out of six is shown. A blot with the C-terminus antibody (bottom) was used to adjust the total amount of GluA1.

(E) Calibration of band density and amount of phosphorylated protein. The densitogram reading was normalized by the 10% phosphorylated sample. Squares are averages of 6 samples.

(F) GluA1 phosphorylation in different subcellular fractions. The fractions from adult rat hippocampi were subjected to SDS-PAGE or Phos-tag SDS-PAGE and blotted with an anti-GluA1 C-terminus. The amount of total GluA1 is preadjusted by performing a separate blot (not shown).

(G) Comparison of intracellular and neuronal surface GluA1 phosphoisotypes. The surface fraction was obtained from dissociated neuronal cultures by surface biotinylation and avidin pull down. The remaining fraction was used as the intracellular fraction.

(H) Ontogeny of GluA1 phosphorylation from P1 to adult hippocampus. Hippocampal homogenate from animals at various ages was separated by conventional and Phos-tag SDS-PAGE and blotted with indicated antibodies. We used the N-terminus antibody because the C-terminus antibody produced a non-specific band in the P1 sample (not shown). Also, the uppermost band with * in the pT840 blot represents cross-reactivity as it was not detected with the N-terminus antibody. See Fig. S2C for identification of phosphoisotypes. The amount of total GluA1 is preadjusted by performing a separate blot (not shown).

(I) Quantification of phosphorylation in P1 hippocampus. The level is expressed as adult levels as one. The original image is in Fig. S2B. The level of pT840 may be an overestimation due to cross-reactivity shown with * in the pT840 blot in Fig. S2B. N=5.

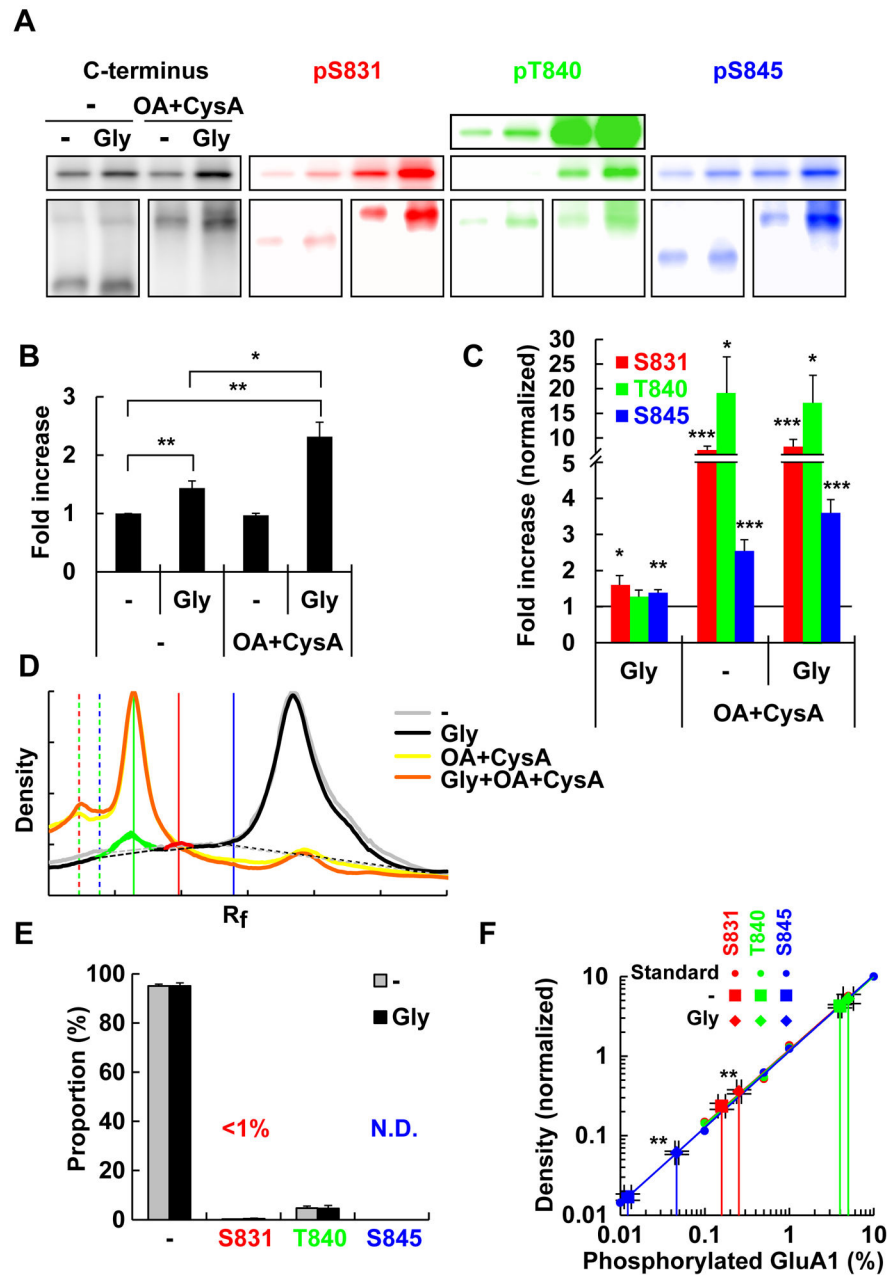


Figure 3. Glycine-induced chemical LTP increases phosphorylation of cell surface GluA1 but the absolute proportion of the phosphorylated population is low

(A) Dissociated neuronal cultures were treated with glycine to induce chemLTP in the absence (–) or presence of okadaic acid and cyclosporine A (OA+CysA). Surface GluA1 was obtained by surface biotinylation and avidin pull down. The samples were subjected to SDS-PAGE (top) or Phos-tag SDS-PAGE (bottom) and blotted with indicated antibodies. Each Phos-tag SDS-PAGE blot had a different exposure time and therefore cannot be cross-compared.

(B) Quantification of the surface GluA1 confirms successful induction of chemLTP.

(C) Amount of phosphorylation normalized by the amount of surface GluA1. The level was determined from the density of conventional SDS-PAGE in (A).

(D) The densitometric profile of Phos-tag SDS-PAGE.

(E) Quantification of data in (C). The peaks at S831 and S845 are below the amount that can be confidently quantified.

(F) The amount of phosphorylated GluA1 before and after chemLTP induction plotted on calibration line of the dilution series.

*: $p < 0.05$, **: $p < 0.01$, ***: $p < 0.001$ (two-tailed t-test). $n=6$ for (B) to (F).

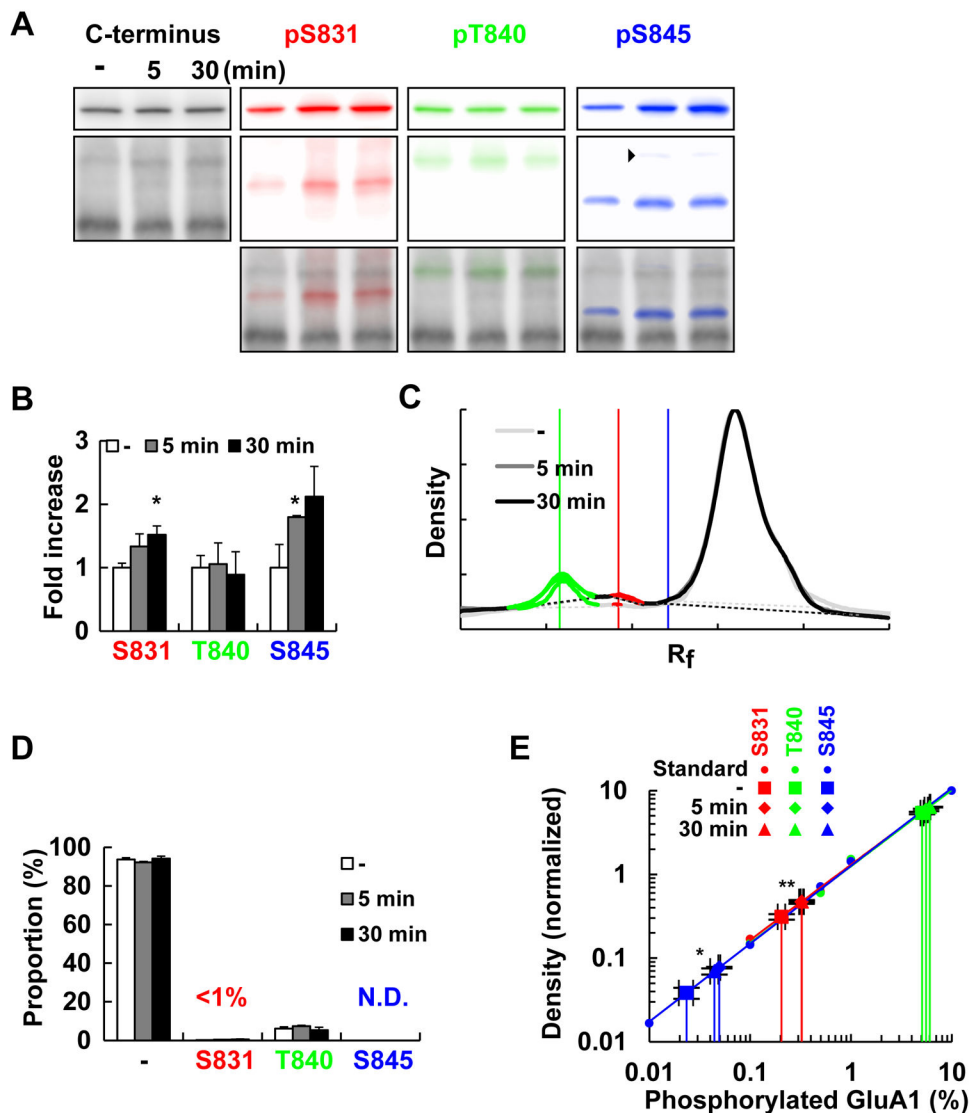


Figure 4. Inhibitory avoidance conditioning increases GluA1 phosphorylation but the absolute proportion of phosphorylated population is low

Rats were subjected to the inhibitory avoidance paradigm. 5 or 30 min after conditioning, dorsal hippocampi were dissected and the fraction insoluble to 1% Triton-X 100 was isolated.

(A) Blotting in SDS-PAGE (top) and Phos-tag SDS-PAGE (bottom). One rat from each group is shown. The top bands (arrowhead) of the pS845 blot (A) most likely represent a dually phosphorylated population at T840 and S845 but because the amount was small (<0.01%), they were not analyzed.

(B) Quantification of phosphorylation using a phospho-specific antibody normalized to the level observed in naïve animals. Blotting in conventional SDS-PAGE was used for the quantification.

(C) The densitometric profile of Phos-tag SDS-PAGE.

(D) Quantification of data in (C).

(E) The amount of phosphorylated GluA1 before and after inhibitory avoidance learning is plotted on calibration line of the dilution series.

*: $p < 0.05$, **: $p < 0.01$ (two-tailed t-test). A total of 9 rats were separated into three groups.